Crack imaging by pulsed laser spot thermography

2010 J. Phys.: Conf. Ser. 214 012072

(http://iopscience.iop.org/1742-6596/214/1/012072)

15th International Conference on Photoacoustic and Photothermal Phenomena (ICPPP15) IOP Publishing
Journal of Physics: Conference Series **214** (2010) 012072 doi:10.1088/1742-6596/214/1/012072

Crack imaging by pulsed laser spot thermography

T. Li[1], D. P. Almond[1], D. A. S. Rees[1], B. Weekes[2]

[a] UK Research Centre in NDE (RCNDE), Department of Mechanical Engineering,
University of Bath, Claverton Down, Bath, BA2 7AY, UK
[b] UK Research Centre in NDE (RCNDE), Imperial College, London, SW7 2AZ, UK

E-mail: D.P.Almond@bath.ac.uk

Abstract. A surface crack close to a spot heated by a laser beam impedes lateral heat flow and produces alterations to the shape of the thermal image of the spot that can be monitored by thermography. A full 3D simulation has been developed to simulate heat flow from a laser heated spot in the proximity of a crack. The modelling provided an understanding of the ways that different parameters affect the thermal images of laser heated spots. It also assisted in the development of an efficient image processing strategy for extracting the scanned cracks. Experimental results show that scanning pulsed laser spot thermography has considerable potential as a remote, non-contact crack imaging technique.

1. Introduction

Conventional optically stimulated transient thermography NDE has been very successful in detecting in plane defects such as delaminations or impact damage in carbon fibre composites [1-4]. However, the approach of generating a thermal transient by high power flash lamps across a broad area of a sample surface is not suitable for the detection of near surface cracks that develop, predominantly, perpendicular to the surface. Pulsed laser spot imaging [5,6] is a technique that uses a high power focused pulsed laser spot to produce a highly localised heating spot from which heat diffuses radially. A crack developed perpendicular to the surface, that is close to the heated spot, will impede the lateral heat flow. A thermal image will reveal the perturbation caused by the crack and this can be used to detect its presence [5,6]. Following the success of the preliminary studies [5,6], a new image processing technique is presented here that results in a direct image of a crack.

2. A 3-D thermal model for cracks

The new technique arose from results obtained from modelling the interaction between a laser induced heat spot and a crack. A 3-D numerical heat transfer model has been developed that has the ability to deal properly with heat flow though air filled cracks with openings in the micrometre range. This is achieved by balancing thermal fluxes flowing into the crack and through the crack, with those flowing out of the crack. Thermal 'ghost points' are generated in the numerical modelling mesh that guarantee correct thermal gradients in the bulk material either side of the crack [5,6]. This avoids the need of the very fine mesh spacing that is necessary to deal with real cracks that often have openings of only a few micrometres. Compared with other heat transfer 3D models based on the finite difference method, there are great savings in computation time and memory.

The parameters that are found by the model to affect the thermal images include: host material, crack opening, length depth and geometry; laser power and pulse duration; spot imaging time and spot distance from the crack. Firstly, a pulsed laser spot was chosen to excite the thermal transient because a bigger temperature difference will be produced across the crack using a short laser pulse. If the pulse is long, heat will start to dissipate in the sample whilst the laser is still on. This phenomenon is more obvious in metal samples. Figure 1a shows the modelled surface temperature image of a laser beam incident on a stainless steel metal block obtained from this 3-D model. This thermal image was obtained 0.15 seconds after the block was irradiated by a 21watt, 50ms laser pulse with radius of 1mm (1/e fall) at the right hand side of a crack (laser spot centre was 1mm away from the crack). In the middle of the metal block, a 5mm long half penny crack was embedded in the grids. Crack opening was 1µm. Thermal flow in the image is shown as a 'D' shape rather than a round shape because of the heat blockage by the crack. Figure 1b shows the temperature profile across the crack and the centre of the spot.

Based on both experimental and numerical simulation results, the 'optimum' imaging distance of the laser spot centre from the crack was found. It is one radius of the spot size. For a spot with Gaussian shape in space, the radius means 1/e fall position. The 'optimum' distance is where the temperature difference across the crack has the largest value. Thus the crack will block heat flow more obviously. Figure 2a shows the temperature difference across the crack when the spot centre has different distances to the crack. At the position of 0.8mm, which is 1 radius (1/e fall) of the Gaussian shape spot, it reaches the biggest value. Furthermore, 'optimum' viewing time at the optimum distance can also be determined if the full length of the crack is required to be revealed above the noise. In our experiments, the 'optimum' viewing time happened at the 12th frame, for example for a 3mm long, 10µm wide half-penny crack in an Udimet test-piece, when the frame rate was 60Hz.

The following conclusions have been derived from the modelling results, though they need to be validated by further experimental investigations:

1. A 1mm long half penny crack with crack opening of 1µm can still be detected if the background thermal noise is within 0.5K.
2. The full length of a crack in mild steel will not be exposed for one spot irradiation if it is longer than 3 times of the spot radius.
3. The temperature difference across the crack reaches a plateau value for crack parameters greater than: 2.5mm in length, 2mm in depth and 2µm in opening when the crack is in a mild steel metal block and the laser spot radius is around 1mm. An example of these dependences is Figure 2b showing the variation of the temperature difference across a crack with different crack opening.
4. Scanning step determination relates with the signal to noise ratio. For a 1mm half penny crack with opening of 10µm in metal samples, the scanning step can be large as 2mm to reveal the crack in our experiments.

In addition, this 3-D model helped to develop a new crack imaging method. A common image processing technique is to compute the first spatial derivative which reflects the amplitude change rate in an image and thus extracts the edge effect in an image. However, the background heat flow caused by the laser spot is still strong and mixed together with the crack when the spot is close to the crack. The 'second derivative' was considered in our experiments since it can further enhance the edge effect in an image. Figures 3a and 3b respectively are the first and second derivative images of the data shown in Fig. 1a.

More thermal images at different times can be used to sum together to further emphasize the invariant crack structure and average the changed background heat flow. However, the 'second-derivate' method is sensitive to the thermal noise [7]; so only thermal images with high signal to noise ratio should be considered. After adding in ±0.5K random thermal noise in the above model, summed absolute second derivative thermal image in x direction from 0.05s (after laser spot was off to reduce the obvious background heat flow in the beginning) to 0.3s (after 0.3s, signal to noise ratio is relatively poor) was derived as Fig. 3c. The revealed crack length above the noise level was smaller than 5mm (about 3.8mm long) because of the heat dissipation. The full length of crack can be revealed by the raster scanning method used below.

3. Experimental results

A stainless steel test-piece [8] containing an 11mm long, 3mm deep crack with average opening of 24.5μm was raster scanned using 21watt, 50ms laser heating pulses. The laser spot radius was 1mm (1/e fall) and the IR camera field of view was 26.4×20.6 mm. Using the above image processing method plus subtracting the background noise, summed second derivative images were obtained as Figures 4a and 4b. The difference between them is that they show second derivative images in x (320 pixels) and y (250 pixels) directions respectively. These images are in good agreement with the dye penetrant image of the crack shown in Fig. 4c.

As aforementioned, this laser spot imaging method is sensitive to noise like other second derivative methods. In addition, other features than the crack will also been imaged, such as dent marks on the surface. Despite these limitations for this technique, it provides a new quick examination method for near surface micron cracks. The sensitivity and reliability of this technique for industrial application is being investigated. At present, a 5mm long crack in an Udimet test-piece with the opening of less than 1μm can be detected and imaged by this technique.

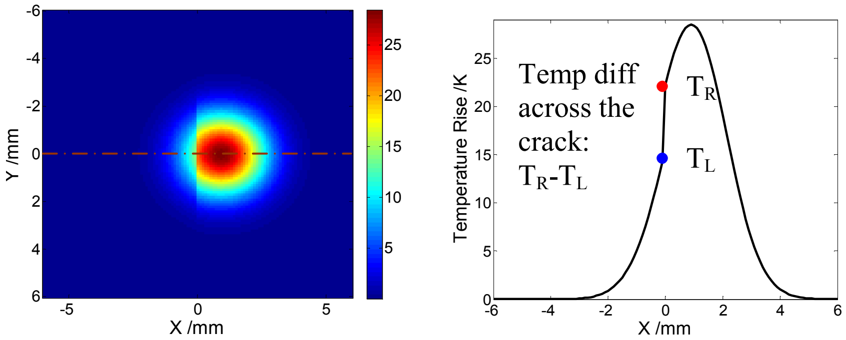

(a) **(b)**

Figure 1. (a) Simulated thermal image with embedded 5mm half penny crack at time 0.15s. (b) Temperature profile across the crack and the centre of the spot.

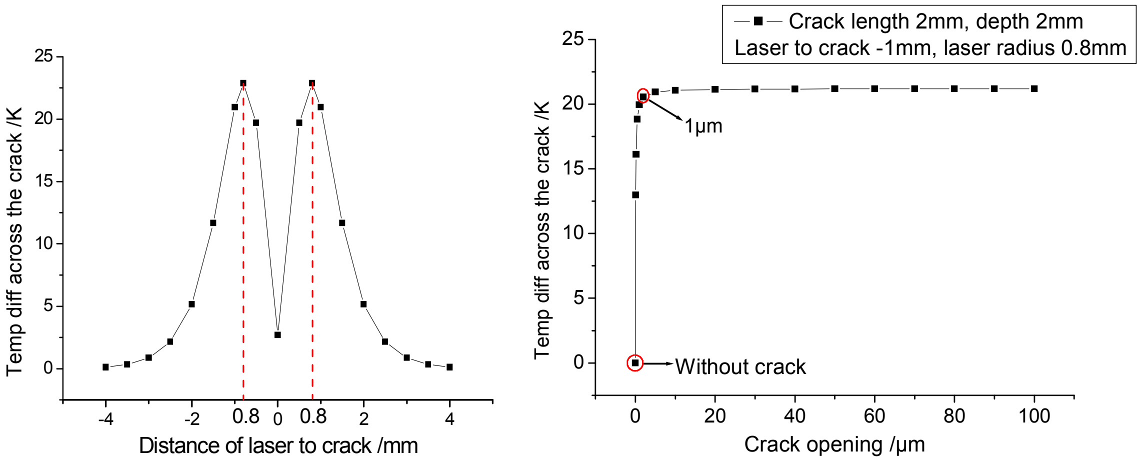

(a) **(b)**

Figure 2. Temperature differences across the crack (a) when the spot centre has different distances to the crack; (b) when the crack opening has changed.

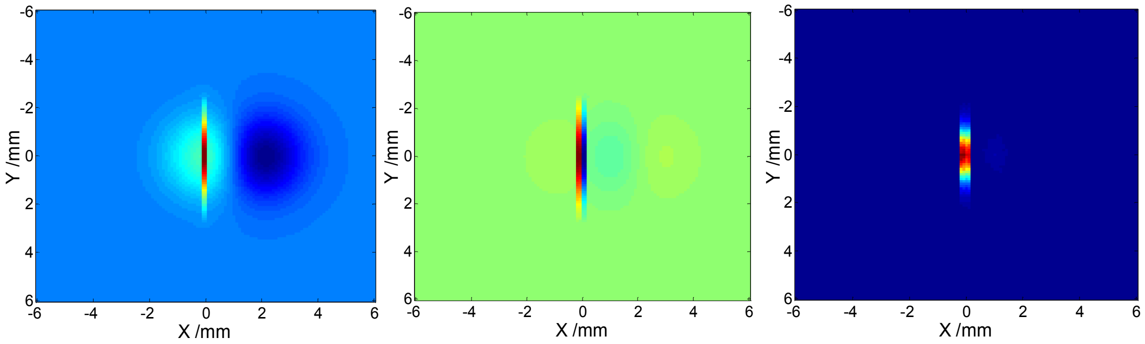

(a) **(b)** **(c)**

Figrue 3. (a) First derivative image in x direction from Figure 1a. (b) Second derivative image in x direction from Figure 1a. (c) Summed second derivative image in x direction from 0.05s to 0.3s.

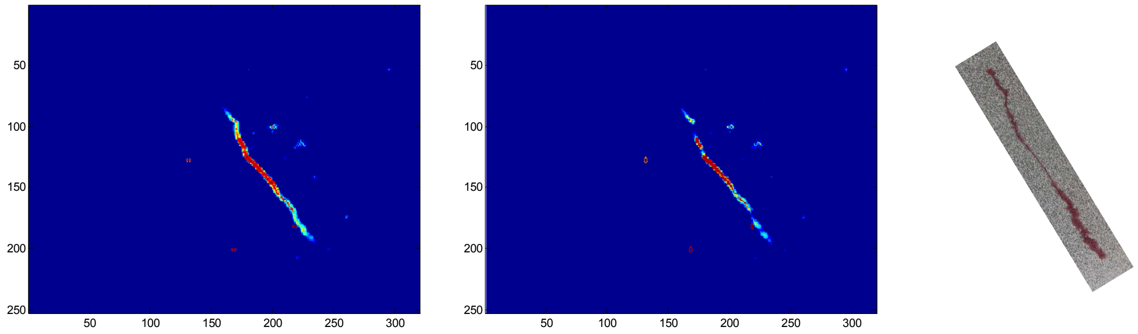

(a) **(b)** **(c)**

Figure 4. (a) Second derivative image in x direction. (b) Second derivative image in y direction. (c) Dye penetrant image of the crack.

Acknowledgement

This research was funded as a targeted research project of the Engineering and Physical science Research Council (EPSRC) UK Research Centre in NDE (RCNDE). The work also received support from Rolls Royce plc, RWE Npower and the National Nuclear Laboratory.

References

[1] W. N. Reynolds, Can. J. Phys. **64**, 1150 (1986).
[2] J. M. Miline& W. N. Reynolds, Proc. SPIE **52**, 119 (1984)
[3] S. K. Lau, D. P. Almond, and J. M. Miline, NDT&E Int.**24**, 195-202 (1991).
[4] S. M. Shepard, J. R. Lhota, and T. Ahmed, Nondestructive Testing and Evaluation **22**, 113 (2007)
[5] A. Rashed, D. P. Almond, D. A. S. Rees, S. E. Burrows and S. Dixon, Rev Quantitative NDE **26** ed. D. O. Thompson and D. E. Chimenti, 500-506 (2006).
[6] S. E. Burrows, A. Rashed, D. P. Almond and S. Dixon, Nondestructive Testing and Evaluation **22**, 217-227 (2007).
[7] R. C. Gonzalez , R. E. Woods, Digital Image Processing (3rd Edition), Prentice-Hall, Inc., Upper Saddle River, NJ (2006)
[8] Trueflaw Ltd, Espoo, FI-02330, Finland.